Published paper

Hernandez-Castillo, L.E., Beynon, J.H., Pinna, C., and Van Der Zwaag, S. Micro-scale strain distribution in hot-worked duplex stainless steel. *Steel Research International*, 76, 2-3 (2005), 137-141.

Micro-scale strain distribution in hot-worked duplex stainless steel

Luis E. Hernandez-Castillo, John H. Beynon, Christophe Pinna and Sybrand van der Zwaag

Mr. Luis E. Hernandez-Castillo, Ph.D. student, IMMPETUS, Department of Engineering Materials, The University of Sheffield, Sheffield, UK; Prof. John H. Beynon, IMMPETUS, Department of Engineering Materials, The University of Sheffield, Sheffield, UK; Dr. Christophe Pinna, IMMPETUS, Department of Mechanical Engineering, The University of Sheffield, Sheffield, UK; Prof. Sybrand van der Zwaag, Faculty of Aerospace Engineering, Delft University of Technology, Delft, The Netherlands.

Abstract
A modified microgrid technique has been applied to a laboratory-made duplex stainless steel, to simulate experimentally the local state of deformation of the austenite-ferrite microstructure of low-alloy steels subject to intercritical deformation. A sample containing such a microgrid was deformed by plane strain compression at high temperatures under conditions representative of hot rolling processes. The distortion of the microgrid after hot deformation revealed in a quantifiable manner the plastic flow of both phases and different deformation features. The micro-strain distributions measured can be used to validate the models predicting the hot deformation of low alloyed C-Mn steels during intercritical rolling.

Keywords: Microgrid technique, hot deformation, local strain distribution, dual-phase microstructures, intercritical rolling.

Introduction

Intercritical rolling, i.e. rolling in the temperature range of the austenite-ferrite transformation, is usually avoided in C-Mn and related steels since the transformation leads to an uncontrolled decrease of rolling forces and problems with product gauge control and guidance of strip. However, because of the potential of producing new, high performance hot rolled products and the ability to produce thinner hot strip bands for a given maximum rolling force, the deformability of steel in the two-phase region and its effect on the final microstructure and properties has recently become of great importance [1].

In order to benefit from the advantages of intercritical rolling, a number of metallurgical issues need to be understood better. One of those issues is the description of the deformation behaviour of two-phase microstructures (such as those consisting of austenite and ferrite). In the literature, some simulation studies (e.g. Karlsson and Sundström [2]) have described the deformation of a hard phase in a soft matrix, indicating that the soft phase deforms more and at an earlier stage than the hard phase. In a recent finite element (FE) study, Bodin *et al*. simulated the uniaxial compression of the austenite-ferrite microstructures of a low-carbon steel and showed that the strain localisation depends on the phase fraction as well as the phase connectivity [3].

Up to now few experimental studies of the high temperature deformation of austenite-ferrite mixtures have been made to validate these models. Transmission electron microscopy (TEM) and electron back-scattering diffraction (EBSD), among other techniques, have been used to determine the local dislocation density and misorientation as indirect measures of the local plastic strain [4, 5]. Digital image correlation is a deformation measurement technique, which has been used to characterize the strain fields at the micro-scale [6]. However, this technique requires very specialized equipment and software, and extensive computing.

An electron-litographic technique for manufacturing microgrids, developed almost twenty years ago [7], provides a simpler way to directly observe the plastic flow [8], and measure the micro-scale strain distribution in deformed microstructures [9]. This technique could not be applied to deformation conditions representative of hot rolling processes, until a modification by Pinna *et al*. allowed measurement of the local deformation in steel samples at high temperatures up to 1050^{o}C [10]. The aim of this paper is to present such modified microgrid technique as a tool for characterising and quantifying the micro-scale deformation of hot worked austenite-ferrite microstructures.

Experimental Procedure

The material used in this investigation was a laboratory-made duplex stainless steel with a chemical composition of Fe-29.6Cr-11.6Ni-0.37Mn-0.04C-0.02V-0.02Si-0.02Mo-0.02Cu-0.01S-0.005P (wt%). This model alloy consisting of austenite islands in a ferritic matrix (about 50% volume fraction of each phase), was chosen to simulate the microstructure of low-alloy C-Mn steels in the intercritical regime. The dual-phase microstructure in our model alloy is stable down to room temperature, and has a reasonable resistance to oxidation. The base material was heat treated at 1100^{o}C for 4 days to promote an equiaxed grain shape and to increase the size of the austenitic grains.

An electron-litographic technique for manufacturing microgrids, using the procedure developed by Pinna *et al*. [10], has been used to produce a microgrid on the annealed duplex stainless steel. The grid production process can be summarised as follows. First, an electro-sensitive resin was deposited on the surface of a small duplex stainless steel plate (**Figure 1a)**, which microstructure had been already revealed by electro-etching. The coated sample was baked for 30 minutes at 140^{o}C, to promote the adhesion of the resin and improve the mechanical resistance of the film. Then, the resin was irradiated with the electron beam of a scanning electron microscope (SEM), following the pattern of a square grid (**Figure 1b**). After this, the lines of irradiated resin were removed using a specific solvent (**Figure 1c**). Subsequently, the exposed metal was electro-etched using a solution of 40% HNO_3 and water in order to engrave lines along the paths of irradiation (**Figures 1d**). Finally, the remaining resin was removed by chemical dissolution (**Figure 1e**). Scanning settings and magnification of the SEM, during the irradiation of the resin, were chosen to produce a microgrid with a 4.5μm pitch and a uniform line width of less than 1μm.

After producing the microgrid, a low magnification-high resolution image was obtained in the SEM by combining a large series of back-scattered electron images, covering the whole microgrid before deformation. The backscattered electron mode was selected to enhance the contrast of the microgrid lines and to reduce the topographic contrast induced by deformation.

The microgrid engraved at the middle of a small duplex stainless steel plate was prepared to be deformed at high temperature, following the procedure of the plane strain compression (PSC) test modified by Pinna *et al*. [10]. In this process, the standard geometry of the specimen for PSC tests is modified to allow insertion of the microgrid sample in the deformation region. First, a small plate containing the microgrid (**Figure 2a**) was welded to a similar polished piece (**Figure 2b**). Then, the welded ensemble was inserted into a rectangular hole in the centre of the main PSC specimen (**Figure 2c**). Finally, the inserts and specimen were welded together on top and bottom (**Figure 2d**) to protect the microgrid surface from oxidation during the test.

Once the microgrid sample was assembled and welded within the PSC specimen, it was compressed in a regular

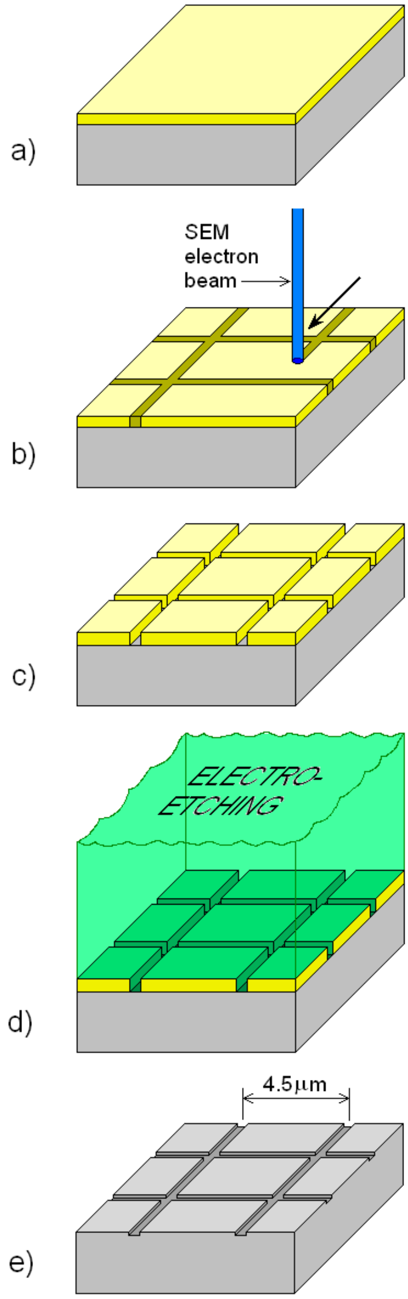

Figure 1. Steps of the modified microgrid technique: a) sample covered with electro-sensitive resin; b) irradiation of resin with the electron beam of the SEM; c) irradiated resin has been removed; d) electro-etching of the exposed metal; e) resulting microgrid.

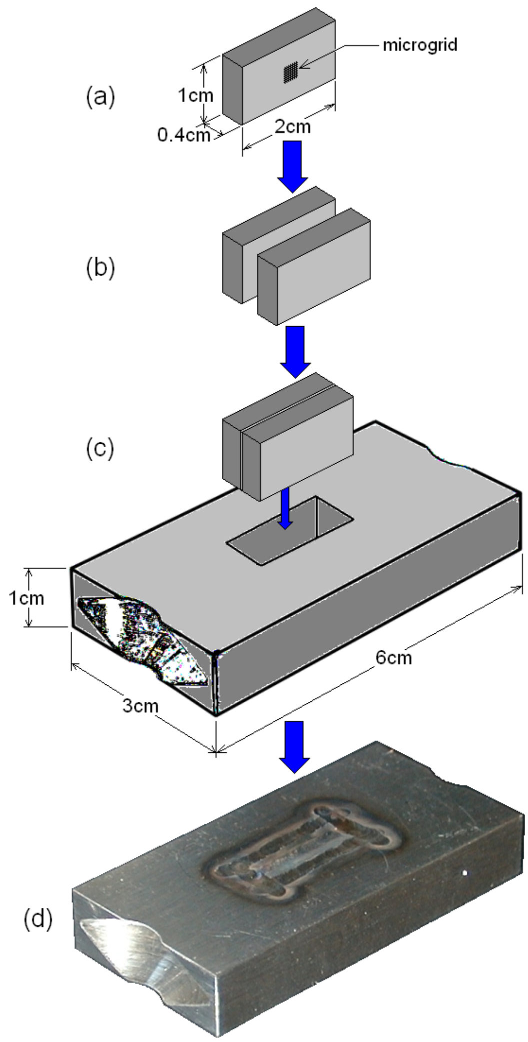

Figure 2. Modified PSC sample assembly: a) micrograds etched on a small plate; b) protection of micrograds with a similar polished plate; c) insertion of ensemble into the main PSC specimen; and d) welded specimen and inserts.

PSC experiment at 850°C to a total strain of 0.3 at $1s^{-1}$ nominal strain rate. Following the hot deformation and water quenching, the microgrid sample was extracted from the PSC specimen, and the entire microgrid was analysed in the SEM, in the same way as before deformation.

Using the grid patterns before and after the deformation at selected locations, several local deformation maps have been produced. The micro-scale strain distribution was calculated using the displacement of the microgrid intersections after deformation. A program developed at the University of Sheffield [11] was used to obtain the coordinates of the undeformed and deformed grids. This program also calculates the Green-Lagrange strain components (e_{11}, e_{22}, e_{12}, e_{eq}) for every square of the deformed microgrid, using the analysis described in [9]. Under the framework of large deformation, the transformation from the undeformed grids to the deformed configuration is characterized by the deformation gradient tensor F. In practice, for each square of the microgrid defined by its four intersection points, we can define two vectors, dX^I ($dX^I(X_1{}^I, X_2{}^I)$) and dX^{II} ($dX^{II}(X_1{}^{II}, X_2{}^{II})$), in the undeformed configuration, and two vectors, dx^I ($dx^I(x_1{}^I, x_2{}^I)$) and dx^{II} ($dx^{II}(x_1{}^{II}, x_2{}^{II})$), in the deformed configuration. From these vectors the in-plane deformation gradient tensor was evaluated, as follows:

$$F=\begin{pmatrix} x_1^I & x_1^{II} \\ x_2^I & x_2^{II} \end{pmatrix}\begin{pmatrix} X_1^I & X_1^{II} \\ X_2^I & X_2^{II} \end{pmatrix}^{-1}$$

The Green-Lagrange strain tensor is then computed as follows:

$$E^{GL}=\frac{1}{2}\left(F^TF\text{-}I\right)$$

where I is the unit tensor and T stands for transposition.

The distribution of the Green-Lagrange strain components was plotted using a surface mapping software to create colour-contour maps. Then, the image of the undeformed microstructure was edited, leaving only the interphase boundaries to be superimposed on the deformation maps, so as to be able to observe where the deformation is distributed with respect to the microstructure.

Results

The modified microgrid technique was successfully applied to the duplex stainless steel used for this study. The definition of the microgrids was improved through several trials, until a line width thinner than 1μm was achieved (**Figure 3**).

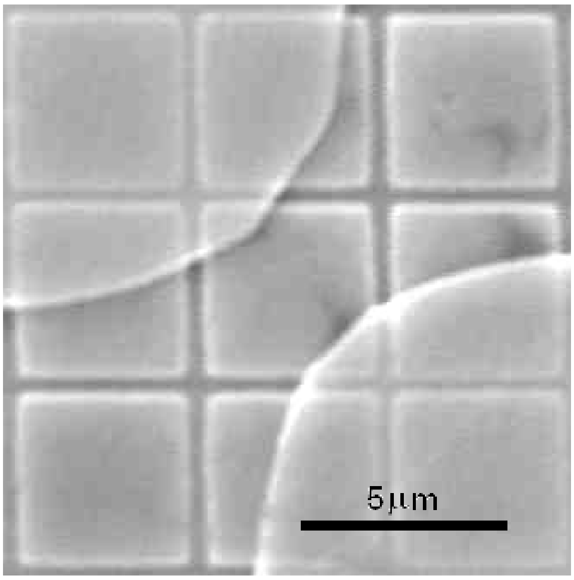

Figure 3. 4.5μm microgrid engraved on duplex stainless steel.

The microgrids produced for this study had an area of about 650x650μm² and a distance between lines of 4.5μm. With the SEM used in this investigation, it would be possible to produce microgrids up to 144μm between lines covering an area of about 10.4x10.4mm².

Low magnification-high resolution images were acquired, covering the complete microgrid before (**Figure 4**) and after deformation, which offer plenty of different scenarios for the analysis of local deformation. The microgrid after deformation was clearly resolvable over its whole area, which is necessary for the SEM analysis and the calculation of strain distribution.

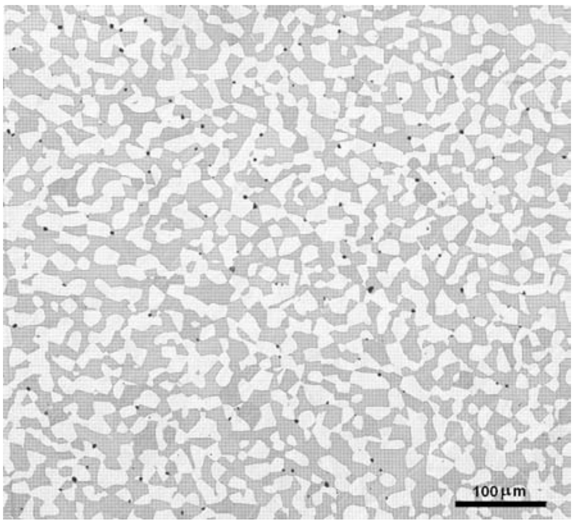

Figure 4. Area covered by the 4.5μm microgrid engraved on duplex stainless steel (lighter phase = austenite).

The SEM analysis allowed direct observation of the plastic flow of both phases after hot deformation, and thanks to the microgrid it is possible to observe and measure the sliding occurring at the interphase boundary, as shown in **Figure 5** by discontinuities of the grid lines.

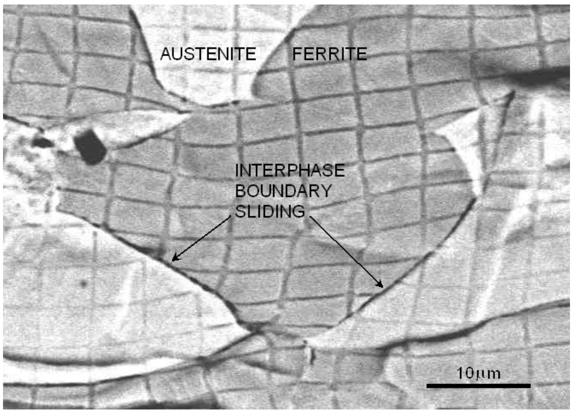

Figure 5. Interphase boundary sliding observed thanks to the discontinuity of the microgrid lines (lighter phase = austenite).

The calculation of the deformation absorbed by each phase, and the measurement of the grain boundary sliding, can be used to study the contribution of the austenite-ferrite interphase boundary sliding to the accommodation of the total strain during hot working.

The displacements of the microgrid intersections were used to calculate and plot several strain distribution maps in small areas covered with the microgrid, such as those shown in **Figures 6** to **8**. The deformation maps indicated larger deformation in the soft ferritic matrix, compared to that in the austenitic phase, in agreement with expectations and model predictions [2, 3].

Discussion

The modified microgrid technique presented here, compared with the classical microgrid technique [7-9], has as a very important advantage the capability to be applied to high temperature experiments. From the results obtained in this investigation it is expected that this technique can be used for larger deformations and higher temperatures, before promoting oxidation on the microgrid surface.

Comparing with other deformation measurement methods such as digital image correlation [6], the modified microgrid technique has the advantage that modest investments in software are required, no specialist hardware is needed, and only a small computer data storage capacity is required. The main disadvantage of this technique is the difficulty of engraving sufficiently fine microgrids. The definition of the microgrids was found to be reduced significantly by even the smallest changes during the procedure.

TEM and EBSD have been used to indirectly measure the local deformation by determining the misorientation in deformed microstructures [4, 5]. The microgrid technique has the advantage, over TEM and EBSD, of allowing direct observation of the plastic flow and measurement of the micro-scale deformation, using the distortion of the microgrid. Another advantage is the

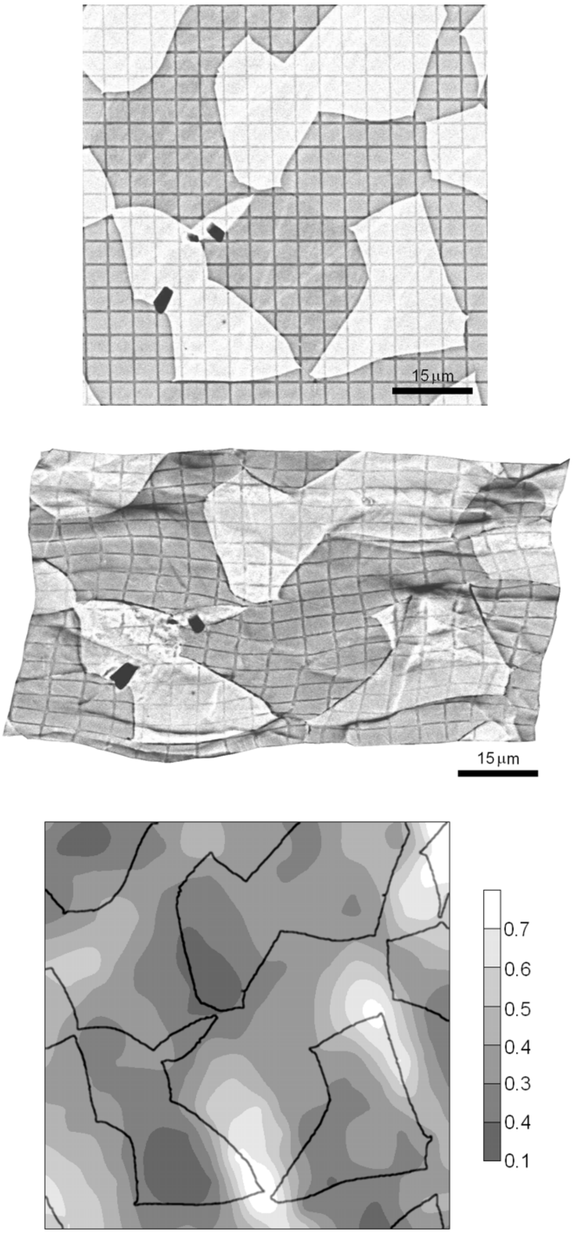

Figure 6. Distribution of Green-Lagrange deformation component e_{11} (deformation in the horizontal direction) in a small area covered by the microgrid (lighter phase = austenite). The average strain values per phase were 0.33 for austenite, and 0.41 for ferrite.

large field analysed, determined by the area of the microgrid. Since this area is large compared with the microstructural length scale (**Figure 4**), there are plenty of locations for detailed strain analysis, enabling the determination of strain patterning at a number of locally different grain morphologies.

Conclusions

The modified microgrid technique has the powerful combination of allowing direct observation and measurement of micro-scale deformation together with the capability to be performed at high temperature. Notwithstanding its potential, the technique requires

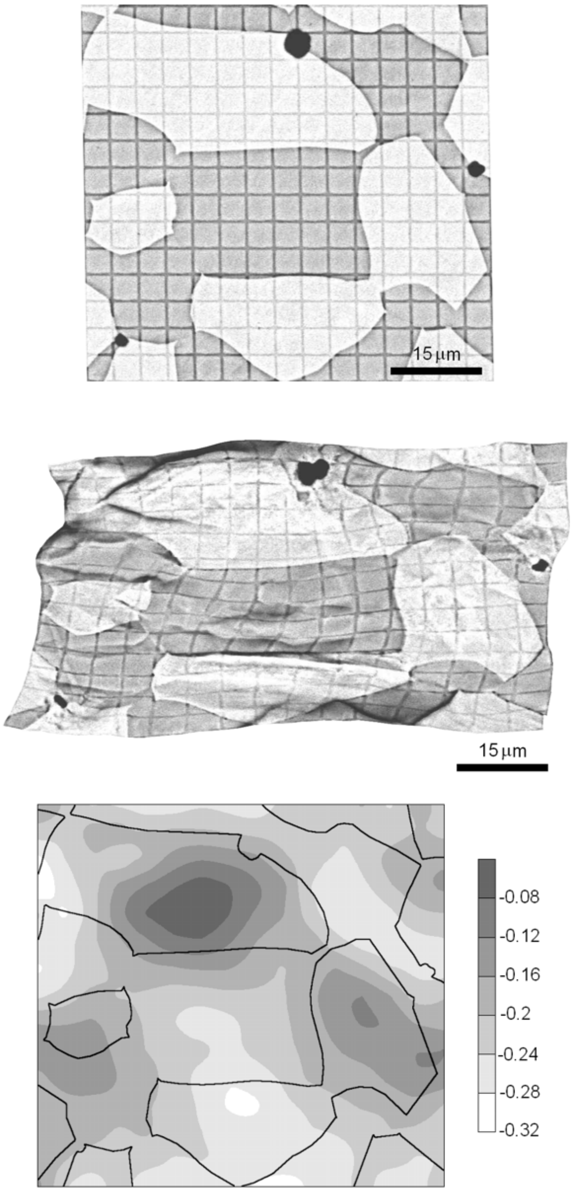

Figure 7. Distribution of Green-Lagrange deformation component e_{22} (deformation in the vertical/loading direction) in a small area covered by the microgrid (lighter phase = austenite). The average strain values per phase were -0.19 for austenite, and -0.22 for ferrite.

relatively simple equipment and computing resources to be performed.

The technique has been successfully applied to duplex stainless steel, producing a well defined microgrid engraved by electro-etching. These microgrids can be deformed at high temperature and then quenched for further characterisation of the deformed microstructure, without evolution of the original austenite-ferrite microstructure (phase transformation or recrystallisation), nor destruction of the engraved microgrid.

The application of the modified microgrid technique to duplex stainless steel opens new possibilities in the study of austenite-ferrite microstructures deformed at high temperature, such as that of low-alloy steel subject to intercritical rolling. Using this technique to calculate the

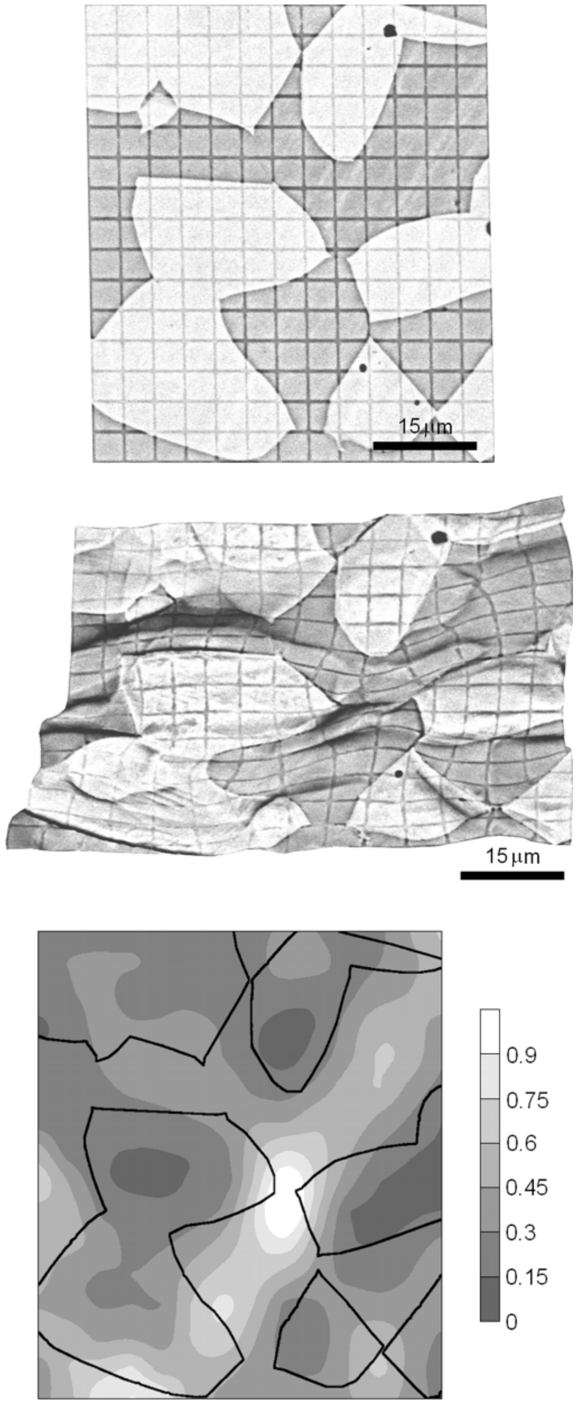

Figure 8. Distribution of Green-Lagrange deformation component e_{eq}, in a small area covered by the microgrid (lighter phase = austenite). The average strain values per phase were 0.31 for austenite, and 0.45 for ferrite.

strain distribution in hot worked duplex stainless steel allows experimental validation of those computer-based models simulating the deformation of austenite-ferrite microstructures, which are the basis to develop approaches predicting the mechanical behaviour of low-alloy steel during the intercritical rolling, and its subsequent microstructural evolution.

Acknowledgments

The authors are grateful to CONACyT and IMMPETUS for the financial support to this project.

References

[1] N. A. Whittaker *et al*., Strain/transformation interaction and mechanical behaviour during intercritical rolling, European Comission report, 2002.
[2] B. Karlsson and B. O. Sundstrom, Materials Science and Engineering, Volume 16 (1974), No. 1-2, p. 161-168.
[3] A. Bodin *et al*., Scripta Materialia, Volume 45 (2001), No. 8, p. 875/882.
[4] C. Y. Barlow and N. Hansen, Acta Metallurgica *et* Materialia, Volume 43 (1995), No. 10, p. 3633/3648.
[5] A. J. Wilkinson and D. J. Dingley, Acta Metallurgica *et* Materialia, Volume 40 (1992), No. 12, p. 3357/3368.
[6] A. Tatschl and O. W. Kolednik, Materials Science and Engineering A, Volume 339 (2003), No. 1-2, p. 265/280.
[7] D. G. Attwood and P. M. Hazzledine, Metallography, Volume 9 (1976), No. 6, p. 483/501.
[8] A. Karimi, Materials Science and Engineering, Volume 63 (1984), No. 2, p. 267/276.
[9] L. Allais *et al*., Acta Metallurgica *et* Materialia, Volume 41 (1994), No. 11, p. 3865/3880.
[10] C. Pinna *et al*., Experimental investigation and micromechanical modelling of the hot deformation of duplex stainless steel, Proceedings of the International Conference on mathematical modelling in metal processing and manufacturing, 2000, Canadian Institute of Mining, Metallurgy and Petroleum, CD only.
[11] Gaëtan Gutierrez, Prediction of deformation and texture evolution in hot rolling of aluminium slabs, internal report-IMMPETUS, 2004.